CR-102665

BOLT BERANEK AND NEWMAN INC

CONSULTING · DEVELOPMENT · RESEARCH

Report No. 1775

3 April 1969

N-I

AN ANALYSIS OF THE NOISE REDUCTION OF ORTHOTROPIC CYLINDRICAL SHELLS

E.K. Bender

Prepared for:

George C. Marshall Space Flight Center
National Aeronautics and Space Administration
Huntsville, Alabama 35812

Attention: Mr. Lawrence Garrison

CAMBRIDGE NEW YORK CHICAGO LOS ANGELES

Report No. 1775 3 April 1969

AN ANALYSIS OF THE NOISE REDUCTION OF ORTHOTROPIC CYLINDRICAL SHELLS

E.K. Bender

BOLT BERANEK AND NEWMAN INC
50 Moulton Street
Cambridge, Massachusetts 02138

Final Report
Contract No. NAS8-20026

Prepared for:
George C. Marshall Space Flight Center
National Aeronautics and Space Administration
Huntsville, Alabama 35812

TABLE OF CONTENTS

	page
LIST OF FIGURES	iii
ABSTRACT	iv
CHAPTER 1. INTRODUCTION	1
2. GENERAL NOISE REDUCTION RELATION	1
2.1 Mode Classes and Energy Balance	1
2.2 Mean-Square Pressures and Acoustical Parameters	5
3. MODAL DENSITIES AND RADIATION RESISTANCES	7
3.1 Approach	7
3.2 Structural Resonances	7
3.3 Regions in Wavenumber Space	9
3.3.1 Frequency region below ring frequency ($0 < f < f_r$)	9
3.3.2 Frequency region between ring and axial critical frequencies ($f_r < f < f_{c1}$)	11
3.3.3 Frequency region between axial and circumferential critical frequencies ($f_{c1} < f < f_{c3}$)	11
3.3.4 Frequency region above circumferential critical frequency ($f > f_{c3}$)	12
3.4 Lengths of Structural Loci	12
4. CONCLUSIONS	14
REFERENCES	17

LIST OF FIGURES

page

Figure 1. Acoustic Power Flow Between Mode Classes 2

2. Loci of Constant Frequency in k-Plane. 10

ABSTRACT

The equations for the noise reduction by an orthotropic cylindrical shell are presented in this report. Statistical energy methods (for resonant mode transmission) and classical methods (for non-resonant mode transmission) are used to estimate the acoustic power flow from a diffuse external noise field to the internal frequency ranges is discussed, showing that noise reduction (NR) will be small for frequencies below the ring frequency and above the highest critical frequency. Between the ring frequency and the lowest critical freqency NR is high and is moderate for frequencies between the lowest and highest critical frequency.

AN ANALYSIS OF THE NOISE REDUCTION OF CYLINDRICAL SHELLS

1. INTRODUCTION

A rocket vehicle generates high-intensity acoustic fields, particularly during its initial launch phase. This external noise environment is transmitted through the vehicle structure to the interior spaces, where it it may have potentially serious adverse effects on personnel and equipment. One needs to know the "noise reduction" (NR) of vehicle structures in order to predict the internal noise levels from external acoustic levels.

Liquid-fueled launch vehicles are typically constructed of rings and stringers, covered with a sheet-metal skin – and may be modeled as an orthotropic cylindrical shell (with different wall stiffnesses in the axial and circumferential directions, depending on the effects of the rings and stringers). This report, accordingly, presents the results of a study of the NR of orthotropic cylindrical shells.

2. GENERAL NOISE REDUCTION RELATION

2.1 Mode Ceases and Energy Balance

One may visualize four mechanisms, as shown in Fig. 1, for the transmission of sound (in a given frequency band) through a structure. An external sound field excites structural modes that are resonant or nonresonant (within the frequency band) and "acoustically fast" (AF) or "acoustically slow" (AS), and each type of mode may contribute to the interior sound field.

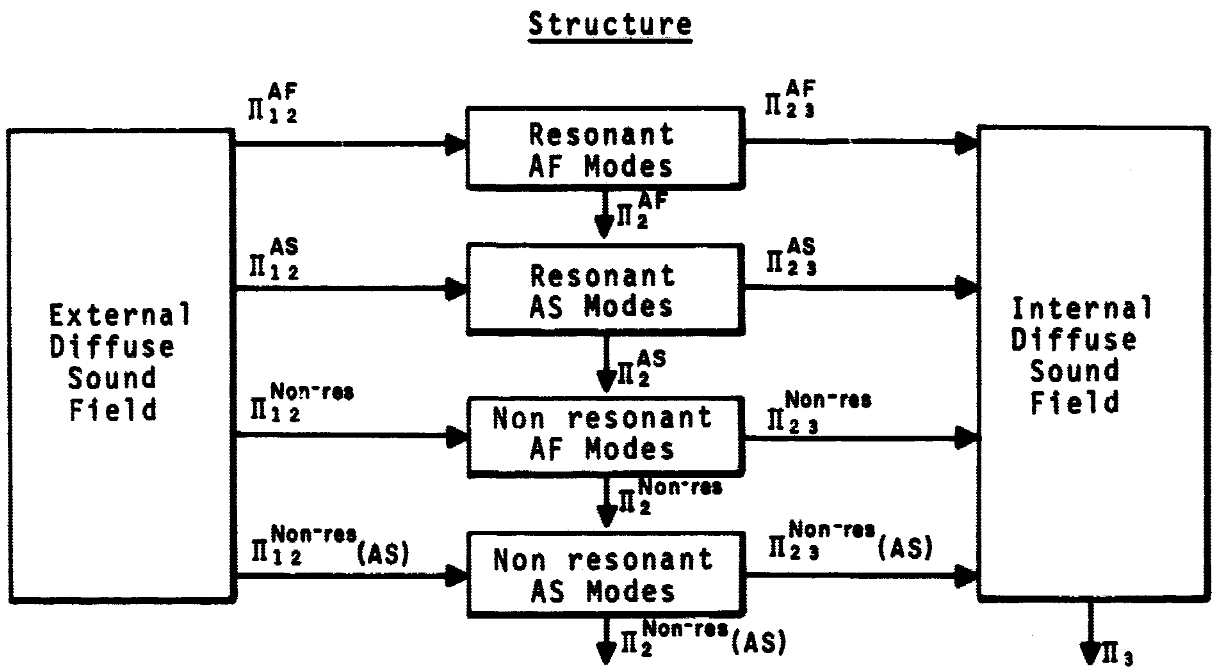

FIG.1 ACOUSTIC POWER FLOW BETWEEN MODE CLASSES

AF modes are those for which the speeds of the flexural wave components that are superposed to from standing waves, are greater than the speed of sound in the adjacent fluid. Analogously, the wave speeds associated with AS modes are subsonic. AF modes radiate sound from the entire shell surface, whereas AS modes radiate only from scattering elements, such as edges [1]. The resonant modes are excited to much larger amplitudes than the nonresonant modes, which are either "stiffness-controlled" or "mass-controlled" (depending on whether the modal resonant frequency lies above or below the excitation frequency respectively).

Because nonresonant, acoustically slow modes contribute very little to noise transmission, we may neglect their effects. The energy balance equations for the other three mode types of Fig. 1 may be written [2–4]

$$\Pi_{12}^{AF} = \Pi_{2}^{AF} + \Pi_{23}^{AF} \tag{1a}$$

$$\Pi_{12}^{AS} = \Pi_{2}^{AS} + \Pi_{23}^{AS} \tag{1b}$$

$$\Pi_{13}^{\text{Non Res}} = A\tau\,(I_1 - I_3)\ , \tag{1c}$$

where Π_{ij} designates power flow from the *ith* to the *jth* element, Π_i designates power dissipated by the *ith* element; A represents the cylinder area, τ the sound transmission coefficient (ratio of transmitted to incident power), and I the intensity (power/unit area of the incident acoustic field). For nonresonant transmission we have assumed that $\Pi_2^{\text{Non Res}}$ is negligible, so that $\Pi_{12}^{\text{Non Res}} = \Pi_{23}^{\text{Non Res}} \equiv \Pi_{13}^{\text{Non Res}}$.

In the steady state, the total power delivered by all three mechanisms must equal the power dissipated in the internal acoustic space; i.e.,

$$\Pi_{23}^{AF} + \Pi_{23}^{AS} + \Pi_{13}^{Non\ Res} = \Pi_3 \ . \qquad (2)$$

The power flow from one group of resonant modes (i) to another (j) is given by [2]

$$\Pi_{ij} = \eta_{ij}\omega n_i(E_i/n_i - E_j/n_j) \qquad (3)$$

where η_{ij} is the coupling factor, n_i and n_j represent the modal densities (number of modes per unit frequency internal) in elements i and j, E_i and E_j denote the energy levels in elements i and j, and ω represents the center frequency of the mode group under consideration.

The power dissipated by resonant modes is given by [2]

$$\Pi_i = \eta_i\omega E_i \ , \qquad (4)$$

where η_i is the dissipation loss factor of the i^{th} element in the frequency band under consideration.

By combining Eqs. 1–4 and using the relation [2]

$$\eta_{ij}n_i = \eta_{ji}n_j \qquad (5)$$

and the assumptions that (1) the structural modes are coupled to the internal acoustic spaces the same as to the external ones (i.e., $\eta_{21} = \eta_{23} \equiv \eta_{sa}$), and (2) that the dissipation loss factors for AS and AF structural modes are the same (i.e., $\eta_2^{AF} = \eta_2^{AS} \equiv \eta_2$), we obtain

$$\eta_{sa}^{AF}\, n_2^{AF} \left[-\frac{E_3}{n_3} + \frac{1}{2+\eta_2/\eta_{sa}^{AF}} \left(\frac{E_1}{n_1} + \frac{E_3}{n_3} \right) \right] + \eta_{sa}^{AS}\, n_2^{AS}$$

$$\times \left[-\frac{E_3}{n_3} + \frac{1}{2+\eta_2/\eta_{sa}^{AS}} \left(\frac{E_1}{n_1} + \frac{E_3}{n_3} \right) \right] + A\tau(I_1 - I_3) = \eta_3\, E_3 \; . \qquad (6)$$

2.2 Mean-Square Pressures and Acoustical Parameters

The energy in an acoustic space of volume V is proportional to the mean square pressure $\langle p^2 \rangle$ [3]:

$$E = \langle p^2 \rangle \, V/\rho c^2 \; , \qquad (7)$$

where ρ represents the density of the acoustic medium and c the speed of sound in it. The modal density of an acoustic space obeys [5]

$$n = \omega^2 \, V/2\Pi c^3 \; , \qquad (8)$$

and the intensity of an acoustic field is given by [6]

$$I = \langle p^2 \rangle / 4\rho c \qquad (9)$$

The dissipation loss factor η_3 for the internal acoustic space (as readily derived from Eq. 11.14, [7]) is related to the mean absorption coefficient α_3 of A_3 (i.e., of the total area of the surface that encloses that space) by

$$\eta_3 = \frac{c A_3 \overline{\alpha}_3}{4\omega V_3} \; . \qquad (10)$$

Solving for $\langle p_1^2 \rangle / \langle p_3^2 \rangle$ after substituting Eqs. 7–10 into Eq. 6 we find

$$\frac{\langle p_1^2 \rangle}{\langle p_3^2 \rangle} = \frac{\left[\frac{\left(1 + \eta_2/\eta_{sa}^{AF}\right) \eta_{sa}^{AF}\, n_3^{AF}/A}{2 + \eta_2/\eta_{sa}^{AF}} + \frac{\left(1 + \eta_2/\eta_{sa}^{AS}\right) \eta_{sa}^{AS}\, n_2^{AS}/A}{2 + \eta_2/\eta_{sa}^{AS}} \right] \frac{2\Pi c^2}{\omega^2} + \frac{\tau}{4} + \frac{\overline{\alpha_3}}{4\omega}}{\left[\frac{\eta_{sa}^{AF}\, n_2^{AF}/A}{2 + \eta_2/\eta_{sa}^{AF}} + \frac{\eta_{sa}^{AS}\, n_2^{AS}/A}{2 + \eta_2/\eta_{sa}^{AS}} \right] \frac{2\Pi c^2}{\omega^2} + \frac{\tau}{4}} \quad (11)$$

The sound transmission coefficient τ obeys [4]

$$\frac{\tau}{4} = \frac{\rho^2 c^2}{\omega^2 \rho_s^2} \ln \left(1 + \frac{\omega^2 \rho_s^2}{4\rho^2 c^2}\right) , \quad (12)$$

where ρ_s denotes the density (mass per unit area) of the structure.

The coupling factor η_{sa} may be expressed in terms of the radiation efficiency σ_{rad},

$$\eta_{sa} = \frac{\rho c}{\rho_s \omega} \sigma_{rad} . \quad (13)$$

Since $\sigma_{rad}=1$ for AF modes at all frequencies [3], the simple expression

$$\eta_{sa}^{AF} = \rho c/\rho_s \omega \quad (14)$$

applies for all AF modes.

The noise reduction NR is defined simply as ten times the logarithm of the ratio of the mean square pressures:

$$NR = 10 \log_{10} (p_1^2/p_2^2) = SPL_1 - SPL_3 \ , \qquad (15)$$

where $SPL = 20 \log_{10} p$ is the sound pressure level. Thus, Eqs. 11–15 enable us to computer the noise reduction, if we know the modal densities and coupling factors, as well as the various physical parameters that enter these equations.

3. MODAL DENSITIES AND RADIATION RESISTANCES

3.1 Approach

In order to evaluate the modal densities and coupling loss factors required for Eq. 11, one would proceed essentially by taking the following steps: (1) obtain the resonance conditions of the shell, (2) compare the wave speeds of the structural modes with the speed of sound to separate the modes into AF and AS classes, (3) determine the densities of AF and AS modes, and (4) determine the average radiation efficiency for AS modes. Much related work has been carried out by Chandiramani *et al.* [3], who studied the structural response of orthotropic shells. We refer the reader to this report for the derivations, but we shall here extract the information required for our calculations.

3.2 Structural Resonances

The structural resonances may be studied most easily in terms of the wave admittance for an orthotropic cylinder, which is given by [3]

$$H(\underline{k},\omega) = (i_3 a/\rho_s c_3)[(r_b^4/\alpha_3) + \cos^4\theta_m - \nu_3^2]^{-1} \ , \qquad (16)$$

where

$$\alpha_1 = h_1/h$$

$$\alpha_3 = h_3/h$$

$$c_3^2 = c_\ell^2 \alpha_3$$

$$r_m \cos\theta_m = k_1 a \alpha_1^{1/2}$$

$$r_m \sin\theta_m = k_3 a \alpha_3^{1/2}$$

$$r_b \cos\theta_b = k_1 (a\kappa_1)^{1/2}$$

$$r_b \sin\theta_b = k_3 (a\kappa_3)^{1/2}$$

$$\nu_3 = \omega a/c_3$$

$$h = \rho_s/\rho_m \ .$$

Here h_1 is defined as an "effective thickness," so that h_1E denotes the extensional stiffness of the shell in the axial direction (for unit width, measured in the circumferential direction). Similarly, κ_1 is defined so that κ_1Eh represents the flexural rigidity in the axial direction. Similar quantities with subscript 3 are defined analogously, but refer to the circumferential direction. Additionally, E represents the Young's modulus, ρ_m the density, and c_ℓ the longitudinal wavespeed of the shell material ($c_\ell^2=E/\rho_m$); ρ_s denotes the average mass of the shell per unit surface area.

Resonance corresponds to infinite admittance, i.e., to vanishing of the bracketed expression on the right hand side of Eq. 16. The equation obtained by setting the term equal to zero is used to plot constant resonance frequency loci in the wavenumber (k_1,k_3) plane, where one may readily relate the structural resonances to the acoustic locus given by $|k|=\omega/c$.

3.3 Regions in Wavenumber Space

Four representative sets of structural and acoustic loci are plotted in Fig. 2. The modes represented by the structural locus that fall within the area bounded by the acoustic locus and the k_1 and k_3 axes are AF. (Note that $c_{structure}=\omega/k_{structural}$; therefore $k_{structure}<k_{acoustic}$ implies $c_{structure}>c$.) The four frequency regions to be studied are bounded by the "ring frequency" f_r, the axial critical frequency f_{c1}, and the circumferential critical frequency f_{c3} (we assume $f_{c1}<f_{c3}$; a similar analysis applies when $f_{c3}<f_{c1}$). The ring frequency corresponds to the "breathing mode," where the cylinder undergoes uniform expansion and contraction, without flexural deformation. The critical frequency in a stated direction is defined as that frequency at which the flexural wave speed in that direction is equal to the speed of sound.

3.3.1 Frequency region below ring frequency ($0 < f < f_r$)

A representative wavenumber locus for frequencies below the ring frequency is shown in Fig. 2a; both AF and AS modes are present. The AF modes radiate much more efficiently than AS modes and will provide the dominant transmission mechanism. Therefore, we shall neglect n_{AS} and σ_{rad}^{AS}. The total number of AF modes $N_{AF}(\omega)$ up to frequency ω is given by [3]

$$N_{AF}(\omega)/A = \left(\frac{c_3}{c}\right)^2 \left(\frac{\alpha_1}{\alpha_3}\right)^{\frac{1}{2}} [\frac{\pi}{2} - \cos^{-1} \sqrt{\nu_3} - \sqrt{\nu_3(1-\nu_3)}] , \qquad (17)$$

and the modal density may be found from

$$n_{AF}(\omega) = \frac{N_{AF}(\omega_2) - N_{AF}(\omega_1)}{\omega_2 - \omega_1} . \qquad (18)$$

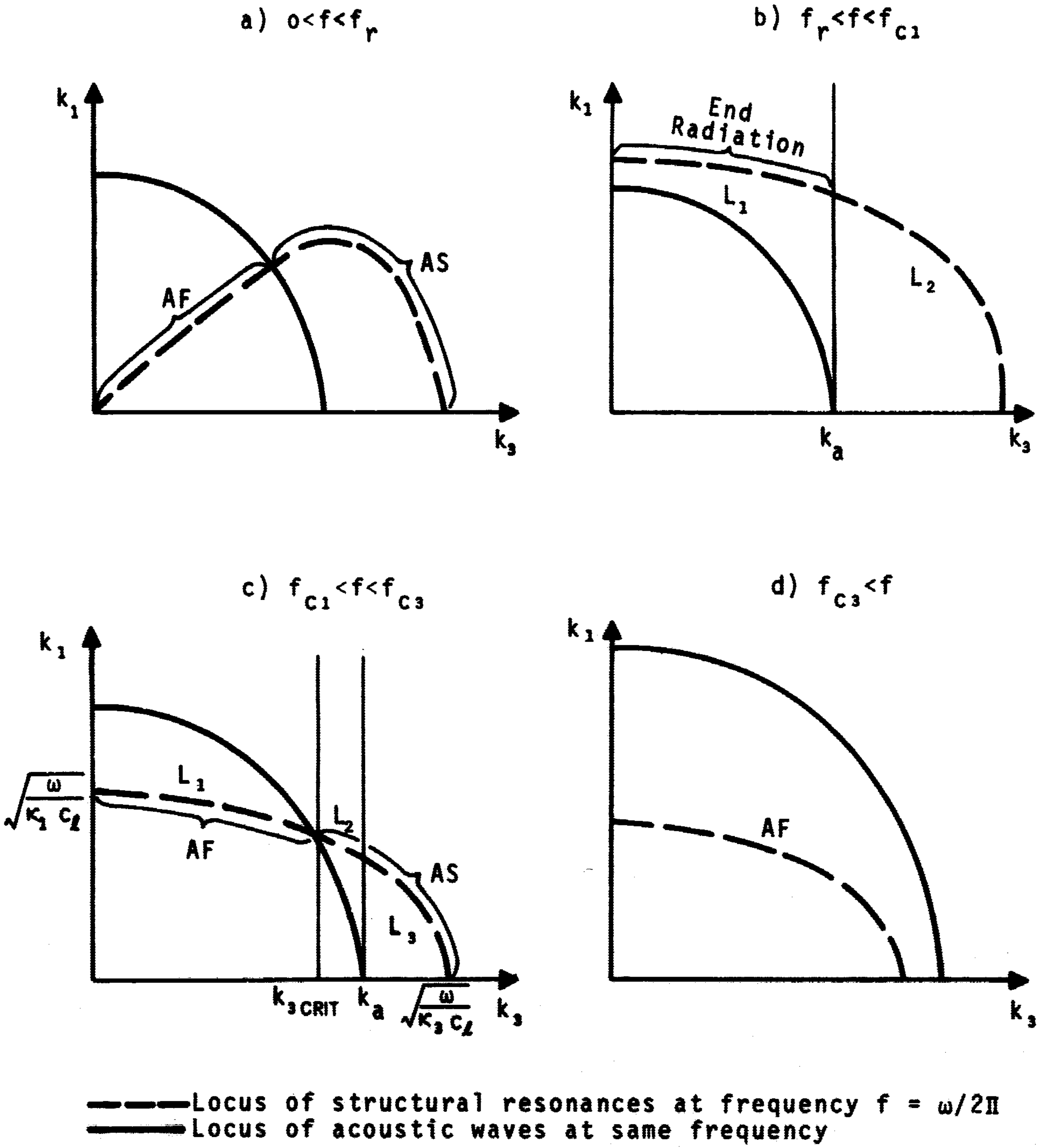

FIG.2 LOCI OF CONSTANT FREQUENCY IN k-PLANE

3.3.2 Frequency region between ring and axial critical frequencies ($f_r < f < f_{c1}$)

Here, the wavenumber loci shown in Fig. 2b apply. There are no AF modes, and radiation by the AS modes is entirely from the ends of the cylinder. The radiation efficiency is strongly dependent on the wavenumbers k_1 and k_3:

$$\sigma_{rad} = (k_a/4\pi a k_1) \quad (2k_1^2+k_3^2-k_a^2)/(k_1^2+k_3^2-k_a^2)^{3/2} \quad . \tag{19}$$

This expression, (which was derived for a plate [1]), must be averaged in order to make it appreciable to a mode group. The modal density for all modes is given by [3]

$$n/A = (4\Pi\sqrt{\kappa_1\kappa_3 c_\ell})^{-1}, \tag{20}$$

and the density of AS modes may be determined by multiplying n by the ratio $L_1/(L_1+L_2)$,

$$n_{AS} = nL_1/(L_1+L_2) \ , \tag{21}$$

where L_1 and L_2 are the lengths of the structural loci corresponding to radiating and nonradiating modes, respectively. (In Sec. 2.3 we derive expressions for these lengths.)

3.3.3 Frequency region between axial and circumferential critical frequencies ($f_{c1} < f < f_{c3}$)

The loci in Fig. 2c show that AF, AS, and nonradiating modes are all present. The radiation efficiency of the AS modes is found here by averaging Eq. 19 along L_2. As usual, the radiation efficiency of the AF modes may be taken as unity. The modal densities are given by

$$n_{AF}/A = (n/A)L_1/L \ , \tag{22}$$

where $L = L_1 + L_2 + L_3$ (see Fig. 2c) denotes the total arc-length of the locus of shell resonances.

3.3.4 Frequency region above circumferential critical frequency ($f > f_{c3}$)

Here, all modes are AF, as illustrated in Fig. 2d. Hence,

$$(n_{AF}/A) = n/A \quad , \quad n_{AS} = 0 \ . \tag{23}$$

3.4 Lengths of Structural Loci

In order to apply to foregoing equations to obtaining an expression for the NR that involves solely structural and acoustical parameters, we need expressions for the lengths of the structural resonance loci illustrated in Fig. 2.

For an orthotropic cylinder, the locus of constant resonance frequency ω is an ellipse given by [3]

$$\omega = \kappa_{1\ell}\kappa_1^{\ 2} + \kappa_{3\ell}\kappa_3^{\ 2} \ . \tag{24}$$

We find L_i by integrating along the ellipse between appropriate boundaries; we obtain a result that may be written as

$$L_i = \int_{\phi_i}^{\phi_{i+1}} \sqrt{1-(1-\kappa_3/\kappa_1)\sin\phi} \tag{25}$$

where the limits of integration are the arc sines of the normalized k_3 coordinates of ends of the segment L_1; the normalization parameter is the value of k_3 corresponding to the intersection of the ellipse with the k_3 axis.

The above integral is an elliptic integral of the second kind and cannot be evaluated analytically. However, numerical values are tabulated in standard mathematical handbooks.

The following expressions for Φ_i are found to apply:

For $f_r<f<f_{c1}$ (Fig. 2b),

$$\Phi_1 = 0 \tag{26a}$$

$$\Phi_2 = \sin^{-1} (\sqrt{\omega\kappa_3 c_\ell}/c) \tag{26b}$$

$$\Phi_3 = \Pi/2 \ . \tag{26c}$$

For $f_{c1}<f<f_{c3}$ (Fig. 2c),

$$\Phi_1 = 0 \tag{27a}$$

$$\Phi_2 = \sin^{-1} (k_{3crit} / \sqrt{\omega/\kappa_3 c_\ell}\ ) \tag{27b}$$

$$\Phi_3 = \sin^{-1} (\sqrt{\omega\kappa_3 c_\ell}\ /c) \tag{27c}$$

$$\Phi_4 = \Pi/2 \ . \tag{27d}$$

For the other two cases, one does not need to know the length of the various loci segments.

The critical wavenumber k_{3crit}, needed for the solution of Eq. 27, corresponds to the intersection of the structural locus (expressed by Eq. 24) and the acoustic locus given by

$$\frac{\omega^2}{c^2} = k_1^2 + k_3^2 \ . \tag{28}$$

Solving Eqs. 24 and 28 gives

$$k_{3crit} = \frac{\omega}{c}\left(\frac{1-\beta_1}{\beta_3-\beta_1}\right)^{\frac{1}{2}} , \tag{29}$$

where

$$\beta_i = c_\ell \kappa_i \omega / c^2 \qquad \text{for } i = 1,3 \ .$$

4. CONCLUSIONS

In this report we have studied the noise reduction of an orthotropic cylindrical shell which has different response characteristics in four frequency regimes. At frequencies below the ring frequency, where membrane stresses dominate, AF modes are present and the shell is fairly well coupled to the surrounding acoustic spaces. Between the ring frequency and the lowest critical frequency (in either the axial or circumferential direction, depending on shell properties) no AF modes are present and NR is large. Between the lowest and highest critical frequencies AF modes are present to varying degrees and the NR is accordingly high or low. For frequencies above the highest critical frequency, where the shell behaves like a plate, all modes are AF and NR is low.

NR equations have been generated in this report and the next step is to use them to compute values of NR for appropriate parameter values. These computations should be performed both for specific shell structures of interest and for a range of parameter values to generate curves and/or tables that one might use to estimate NR functions quickly.

The above analysis relies on certain assumptions which ought to be borne in mind during the application of the formulae generated. One of the assumptions made here is that stiffeners (i.e., rings and stringer) make the cylindrical shell uniformly orthogonal. While this assumption is undoubtedly valid for structural wave lengths that are large compared with inter-stiffener spacing, it is also a poor assumption when wavelengths are far smaller than or approximately the same size as the spacing between stiffeners. For small wavelengths one generally can assume the shell is composed of plates, rigidly supported by the stiffeners [*1,8*]. The problem is most complicated when inter-stiffener spacing and wavelengths are approximately equal in magnitude and a significant effort would be required to develop the state-of-the-art to develop a solution. However, an estimate of response may be made by comparing the results for the cylinder modeled as a homogeneous orthogonal shell and as a collection of plates.

Another significant assumption in applying the above results to launch vehicles is that the acoustic fields are diffuse. This assumption is not especially valid for the highly directional external sound field originating in the turbulent rocket exhaust and impinging on the vehicle through what is probably a shallow angle [*9*]. The internal acoustic field is likely to be reasonably diffuse at high frequencies but is not expected to be diffuse at low freqeuncies where model densities are small [*10–12*].

In order to verify theoretical predictions and to explore areas for which these predictions are of questionable validity, field tests, model experiments and additional theoretical work should be conducted. Physical experiments should provide data that will both test the validity of existing predictive methods and establish a basis for further theoretical studies. The theoretical investigations should be concentrated in the areas where analytical models are known to be invalid (e.g., for directional sound fields and when structural wavelengths are of the same order of magnitude as spacing between stiffness).

REFERENCES

1 G. Maidanik, "Response of Ribbed Panels to Reverberant Acoustic Fields," *J. Acoust. Soc. Am.* **34**, 721-729 (1957).

2. R.H. Lyon, "Random Noise and Vibration in Space Vehicles," Shock and Vibration Monograph SVM-1 (1967).

3. K.L. Chandiramani *et al.*, "Structural Response to Inflight Acoustic and Aerodynamic Environments," Bolt Beranek and Newman Inc Rept. No. 1417 (July 1966).

4. J.E. Manning, R.H. Lyon, and T.D. Scharton, "Transmission of Sound and Vibration to a Shroud-Enclosed Spacecraft," Bolt Beranek and Newman Inc Rept. No. 1431 (Oct. 1966).

5. E.E. Ungar, "Fundamentals of Statistical Energy Analysis of Vibrating Systems," AFFDL-TR-66-52 (Apr. 1966).

6. L.L. Beranek, *Acoustics* (McGraw-Hill Book Co., Inc., New York, 1954).

7. L.L. Beranek, *Noise Reduction* (McGraw-Hill Book Co., Inc., New York, 1960).

8. J.E. Manning and G. Maidanik, "Radiation Properties of Cylindrical Shells," *J. Acoust. Soc. Am.* **36**, 1691-1698 (Sept. 1964).

9. I. Dyer, "Response of Space Vehicle Structures to Rocket Engine Noise," Chap. 7 in *Random Vibrations*, ed. by S.H. Crandall, (The M.I.T. Press, Cambridge, Mass., 1963).

10. R.H. Bolt and R.V. Roop, "Frequency Response Fluctuations in Rooms," *J. Acoust. Soc. Am.* **22**, 280-289 (1950).

11. R.V. Waterhouse, "Statistical Properties of Reverberant Sound Fields," Paper presented to the Acoustical Society of America (Nov. 1963).

12. I.L. Vér, "Feasibility Study for the Diffuse Field Noise Chamber," Bolt Beranek and Newman Inc Rept. No. 1758 (Dec. 1968).